

A Sample Holder for Simultaneous Raman and Neutron Vibrational Spectroscopy

R C Gillis,^{1, a)} Y Q Cheng,¹ F X Gallmeier,¹ M A Hartl,² T Huegle,¹ and E B Iverson¹

¹⁾*Oak Ridge National Laboratory, Oak Ridge, Tennessee, 37831,*

USA

²⁾*European Spallation Source ERIC, Box 176, S-221 00 Lund,
Sweden*

We have built a sample holder (called a center stick or sample stick) for performing simultaneous Raman and neutron vibrational spectroscopy on samples of material at the VISION neutron vibrational spectrometer of the Spallation Neutron Source at Oak Ridge National Laboratory. This equipment holds material samples in the neutron beam within the cryogenic environment of the VISION spectrometer, allowing for samples to be studied at temperatures as low as 5 K. It also provides the capability for gas to be loaded to or evacuated from the sample while it is loaded at VISION. The optical components for directing and filtering light are located within the cryogenic volume, in physical proximity to the sample. We describe the construction of this sample holder and discuss our first measurements of simultaneous Raman and neutron vibrational spectra. The samples that we report on were 4-nitrophenol at a temperature of 20 K, and cryogenic hydrogen of a number of different orthohydrogen fractions.

Keywords: Raman spectroscopy, neutron vibrational spectroscopy, cryogenics, hydrogen, molecular hydrogen, orthohydrogen, parahydrogen, 4-nitrophenol

I. INTRODUCTION

Raman spectroscopy and neutron vibrational spectroscopy (NVS) are frequently employed in materials science. Raman spectroscopy is based on the inelastic scatter of light, and NVS on the inelastic scatter of neutrons. Both are widely used in the investigation of molecular and intermolecular bonding and structure. Raman spectroscopy, given its low cost and portability, is commonly used in the identification and diagnostics of materials.

As the physics that governs the scattering is different for photons and neutrons, these two types of spectroscopy provide complementary information on a material. Raman scattering depends on fluctuations in the electric polarizability and is subject to selection rules determined by symmetries of the molecule. NVS is sensitive to excitations involving atoms that have large neutron-nucleus scattering cross sections, and the fact that this quantity can vary greatly from one isotope to another makes it useful in comparing samples of different isotopic makeup. NVS is particularly sensitive to excitations involving protons as hydrogen has a neutron scattering cross section that is the largest of all elements and an order of magnitude or more larger than most other elements. Also, NVS is not subject to selection rules so can be used to study excitations that are forbidden in optical spectroscopy. For discussions on the strengths and weaknesses of NVS in comparison to other vibrational spectroscopic techniques such as Raman spectroscopy, see e.g. Ref. 1–4. An example of a study that employs the complementarity of Raman, infrared and neutron vibrational spectroscopies is given in Ref. 5.

When exploiting the complementarity of spectroscopic techniques, it is beneficial to perform them simultaneously since the conditions of a sample can be time-consuming or difficult to reproduce. For example, a sample can have a time evolution that depends on a set of

^{a)}Electronic mail: gillisrc@ornl.gov

initial conditions that are difficult to establish with the desired precision. With this consideration in mind, we have built a center stick (also called a sample stick) that incorporates optics for performing Raman spectroscopy *in situ* on samples while they are in place on the VISION neutron vibrational spectrometer of the Spallation Neutron Source (SNS) at Oak Ridge National Laboratory. The setup that we describe in this paper is similar to one that has been in use at the ISIS neutron source of Rutherford Appleton Laboratory,⁶ but is different in two main ways. First, our setup incorporates a large portion of the optics directly within the center stick, in proximity to the sample and within the cryogenic volume of the VISION spectrometer. Secondly, it provides the capability for gas to be loaded to and evacuated from the sample while it is loaded on VISION.

As a demonstration of this equipment, we have performed simultaneous measurements of Raman and neutron vibrational spectra on VISION. The spectra that we report are of 4-nitrophenol and of cryogenic hydrogen of variable orthohydrogen fractions. In section II, we describe the design and construction of this equipment. In section III, we describe the initial measurements.

II. CENTER STICK DESIGN

The Raman probe that we have built was designed for use on the neutron vibrational spectrometer VISION. VISION⁷ is an inverted-geometry inelastic neutron scattering spectrometer. VISION accepts a pulsed white beam with energies ranging from 1 to 2000 meV, and has pyrolytic graphite crystal analyzers and cooled beryllium filters that select neutrons with a final energy of approximately 3.5 meV. There are 14 crystal analyzer arrays, each one consisting of $350 \times 1 \text{ cm}^2$ single crystals arranged on a curved parametric surface that focus the (002) Bragg-reflected neutrons (the beryllium filters suppress reflections of higher order) onto an array of ^3He detectors. There are 7 analyzers oriented in a forward scattering direction (low momentum transfer) and 7 in a backscattering direction (high momentum transfer). The effective energy transfer range of the instrument is from -2 to 1000 meV (-16 to 8000 cm^{-1}). The access to negative energy transfers allows VISION to measure the intensity of the elastic line.

Samples studied with NVS are commonly held at low temperature to reduce the effect of the Debye-Waller factor and thermal broadening of spectral features. The thermal environment of the sample is maintained within a chamber that is referred to as a variable temperature insert (VTI), and which is thermally coupled to a cold head. During cryogenic operation this chamber is filled with helium gas for thermal coupling between the sample container and the inner chamber walls. Samples are loaded to the VTI in a room (the sample environment cave) that is located above the VISION spectrometer. The flange that seals the VTI is at the top of the chamber and at floor level in the sample environment cave.

The support that holds the sample in the neutron beam and seals the VTI from above is referred to as a center stick. Center sticks are loaded to VISION from above and have a vacuum flange that mates with the flange of the VTI. The VTI has an inner height of 120 cm and an inner diameter of 8.5 cm. The neutron beam has a maximum size at the sample position of 3 cm wide \times 5 cm tall and hits the sample area at 110 cm below this mounting flange. The VTI can hold the sample at temperatures as low as 5 K and as high as 700 K. The physical construction of center sticks on VISION can vary based on the requirements of the sample, although cryogenic thermometry and temperature control are standard.

The center stick that we discuss in this paper incorporates Raman optics to allow Raman spectroscopy to be performed simultaneously with NVS on VISION. It could also be used on

This manuscript has been authored by UT-Battelle, LLC under Contract No. DE-AC05-00OR22725 with the U.S. Department of Energy. The United States Government retains and the publisher, by accepting the article for publication, acknowledges that the United States Government retains a non-exclusive, paid-up, irrevocable, worldwide license to publish or reproduce the published form of this manuscript, or allow others to do so, for United States Government purposes. The Department of Energy will provide public access to these results of federally sponsored research in accordance with the DOE Public Access Plan (<http://energy.gov/downloads/doe-public-access-plan>).

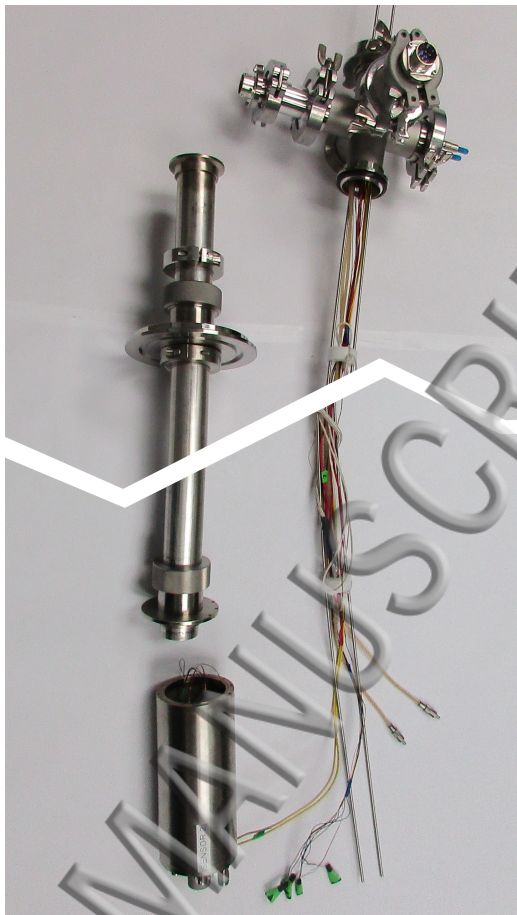


FIG. 1. The support column of the VISION Raman center stick during assembly. When this equipment is fully assembled, the distance from the top of the 6-way cross to the bottom of the vacuum chamber is 130 cm. The outer diameter of the vacuum chamber at bottom left is 7.6 cm.

other scattering instruments that use a VTI and sample container of compatible dimensions. We refer to it in this paper as the Raman center stick. A challenge associated with designing and building the Raman center stick has been the transmission of an optical signal to and from the sample in a cryogenic environment, across vacuum-tight boundaries. Another primary consideration was the space limitation imposed by the 8.5 cm inner diameter of the VTI.

The Raman center stick can be conceptually divided into three parts: a support column, an optical system, and a sample container. The support column provides most of the frame of the center stick, has a flange that seals the VTI while the center stick is loaded, contains the optical components, optical fibers and cryogenic wiring within an evacuated environment, and also contains the gas lines for connecting the sample container to a gas handling system. The interfaces that connect the optics, cryogenic wiring, vacuum and gas lines to external components are located at the top of the support column. The optical system consists of the components that direct light through the center stick from the excitation laser to the sample, and from the sample to the optical spectrometer. A large portion of the optical system within the center stick is located in an assembly of optical components that directs, focusses and filters both the excitation light and the scattered light. The sample container is optically coupled to the optical assembly and attaches to the bottom of the support column. The support column and its associated vacuum components, the optical

system, and the sample container will now be discussed in turn.

Fig. 1 shows a photograph of the support column of the Raman center stick. Shown at the top right corner of this photograph is a 6-way KF-40 cross which provides a connection for a vacuum pump and has feedthroughs for two optical fibers, two gas lines, and wiring for cryogenic thermometry and temperature control. The optical feedthroughs conduct light to and from the optical assembly, which is held inside the 304 stainless steel vacuum chamber shown at the bottom left. The 6-way cross and the vacuum chamber are connected to each other by the stainless steel vacuum tube that is shown at the top left. Near the top of the vacuum tube is the flange that seals the VTI and fixes the center stick in place when it is loaded on VISION.

Fig. 2 shows a schematic of the vacuum chamber and sample container inside the VTI. An optical coupling allows for light to pass between the optics in the vacuum chamber and the sample in the sample container while the sample container, vacuum chamber and interior of the VTI are separated from each other by vacuum-tight seals. Due to space constraints, the gas lines pass through rather than around the vacuum tube and vacuum chamber. The gas lines pass unbroken from the air side of the vacuum feedthrough to the interior of the sample container, through the vacuum tube and vacuum chamber, across the intervening space between the vacuum chamber and sample container, and across the 304 stainless steel lid of the sample container. The sample container itself is made of 6061-T6 aluminum alloy and has walls that are 1 mm thick. This construction allows for sample pressures of well over a bar. The outer walls of the gas lines are sealed at the vacuum feedthrough, vacuum chamber floor and sample container lid by 1/8-inch Swagelok fittings that are fastened with Teflon ferrules. The use of Teflon in place of steel ferrules allows for the positioning of the gas lines to be adjustable.

Cryogenic thermometers and heaters are attached to the optical assembly and to the gas lines inside the vacuum tube. The temperature of the optics is controlled as the optics may have properties that vary with temperature (such as due to a temperature-dependent film thickness), and it is also possible if the vacuum is poor that impurities will accumulate on the optics below a certain temperature. The temperature of the gas tubing is similarly controlled to prevent accumulation of material inside the lines. The bottom of the vacuum chamber also has an electrical feedthrough for connecting cryogenic thermometry to the sample container.

The optical assembly is shown in Fig. 3. The optical assembly is held together by components of the Thorlabs⁸ 16 mm optical cage system, which maintains the alignment of the optical components within the confined space of the vacuum chamber. The excitation port of the optical assembly couples the excitation fiber to the optics by a fiber collimator upstream of a laser line filter. Downstream of the laser line filter, the incoming light encounters two 90° reflections: a mirror followed by a dichroic filter. The mirror and dichroic filter are aligned parallel to each other, and at 45° to the axis of the excitation fiber collimator. The beam incident on the sample is offset from but parallel to the axis of the excitation fiber collimator. Measurements using a laser power meter have shown that this setup transmits about 60 % of the laser power from the upstream side of the excitation port of the optical cage to the sample position. The dichroic filter transmits the down-scattered light from the sample to the collection port, and blocks much of the light of the excitation frequency (or higher) from entering the collection optics. At the collection port, the light encounters a notch filter for final suppression of light of the excitation frequency, followed by a fiber collimator that is aligned parallel to the excitation fiber collimator and coaxially with the excitation beam incident on the sample. We used 200 μm core, 0.22 numerical aperture multimode fibers on the excitation side and 400 μm core 0.39 numerical aperture multimode fibers on the collection side. The laser line filter, dichroic filter and notch filter are for 488 nm light.

For the measurements that are discussed in this paper, the sample container was coupled optically to the optical assembly in the vacuum chamber by a 13 mm diameter fused quartz rod. The quartz rod was sealed at the floor of the vacuum chamber and at the lid of the sample container using 1/2-inch Ultra-Torr vacuum fittings, with indium and Field's metal

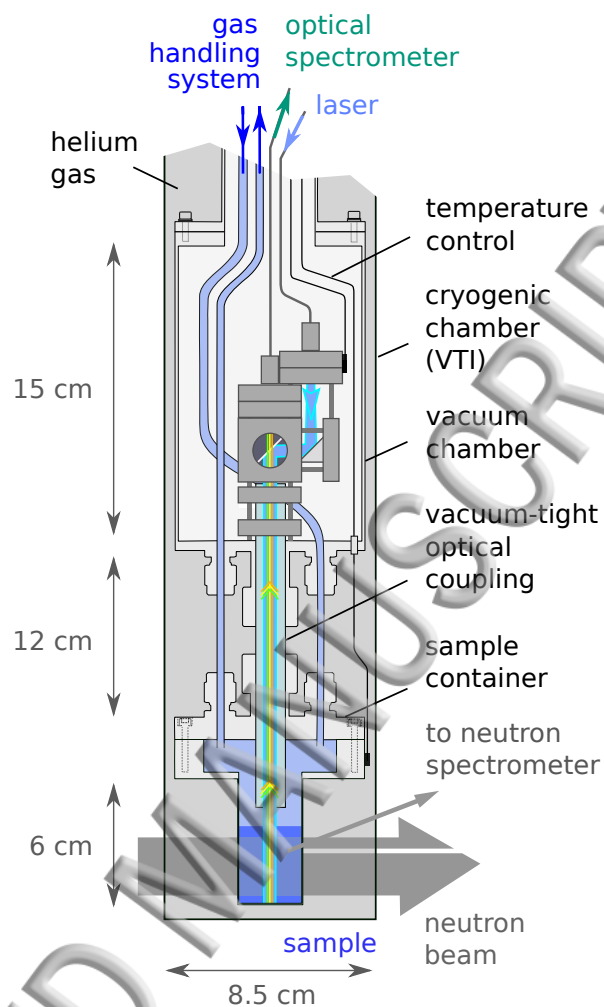


FIG. 2. A view inside the VISION refrigerator while the Raman center stick is loaded. This diagram is approximately to scale in the horizontal direction but compressed in the vertical direction for space reasons.

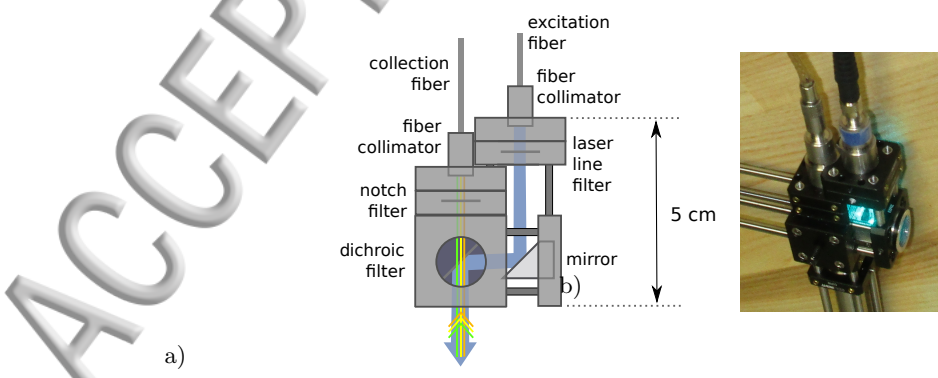


FIG. 3. a) The optical assembly, showing the path of the excitation and collected light. b) A photograph of the optical assembly before it was incorporated into the center stick. The steel rods emerging at bottom and left were used during alignment and were removed before incorporating the assembly into the center stick.

(which we made of 32.5 % Bi, 16.5 % Sn and 51.0 % In by weight) in place of the usual room-temperature rubber o-rings. With this setup, it was possible to attain a vacuum in the range of 10^{-5} mbar, although the vacuum seals at the modified Ultra-Torr fittings were fragile and very difficult to work with. We have also used Torr Seal epoxy at the boundary between the quartz rod and the Ultra-Torr fittings. The sample container was physically attached to the vacuum chamber by this quartz rod and by the 0.3 cm OD stainless steel gas lines. The quartz rod and steel gas lines are shown to be connecting the sample container to the vacuum chamber in this way in Fig. 2.

At the 6-way cross we have used both receptacle-style optical feedthroughs (which allow fibers to be detached) and penetrating feethroughs (which pass fibers unbroken across the vacuum-air boundary). Examples of penetrating feedthroughs are given in Ref. 9–13. We made penetrating feedthroughs by carefully removing the protective plastic from around the fiber, and passing the fiber though a 1/2-inch OD aluminum tube that was later filled with silicone sealant to provide a vacuum-tight seal between the fiber and the inner wall of the tube. The tube was also plugged on the vacuum side with 2216 B/A Gray epoxy for structural reinforcement. The 1/2-inch OD aluminum tube was sealed at the air-vacuum boundary of the six-way cross with 1/2-inch Swagelok fittings and Teflon ferrules. The penetrating feedthrough has the benefit of not suffering transmission losses, but naturally has the drawback that if a fiber breaks on the air side the entire system has to be dismantled to replace it.

The purpose of placing the optical assembly close to the sample is to provide maximum control of backgrounds in the Raman spectrum. In the case of the measurements discussed in this paper, scattering of light by the quartz rod either provided an unimportant background (in the case of 4-nitrophenol which has a very intense Raman signal) or was separable from the signal (in the case of hydrogen). In the case of hydrogen, the background from the quartz rod provides the benefit of allowing us to normalize the Raman signal from the sample to the transmitted laser power (the signal from the sample and from the quartz are both proportional to the laser power, and both are subject to the efficiency factors associated with transmissions and reflections throughout the optical system). In the case where low backgrounds will be desired in the Raman signal, we plan to replace the quartz rod with a quartz tube with a thin window, or to use a flanged optical viewport between the vacuum chamber and the sample container.

Within the vacuum tube and vacuum chamber, the gas tubing, cryogenic wiring, optical fibers and optical assembly were wrapped in seven layers of aluminized mylar insulation. The outer wall of the vacuum tube and vacuum chamber were also wrapped in multiple layers of the same insulation. It was possible to hold the sample at 20 K and the optics at a temperature of at least 125 K with a temperature difference of not more than 1 K between the sample container and the quartz rod at the entrance of the sample container. For the hydrogen study, the optics were held at 50 K, and for the 4-nitrophenol study the optics were held at 125 K. We have not yet attempted to raise the temperature of the optics higher than 125 K.

III. INITIAL MEASUREMENTS

As a first use of the Raman center stick, we have performed simultaneous Raman and neutron vibrational spectroscopy on VISION of 4-nitrophenol, and of a number of samples of liquid and solid hydrogen with variable orthohydrogen fractions. For these measurements we used a 50 mW 488.0 nm CW laser (model Stellar Pro 488/50 by Modu-Laser¹⁴) and an optical spectrometer of model HR2000+ by Ocean Optics.¹⁵ 4-Nitrophenol provides a good demonstration of complementarity of Raman spectroscopy and NVS as it produces a very strong Raman signal, and its most intense features are not visible in the neutron vibrational spectrum. Molecular hydrogen provides a good demonstration of the diagnostic application of Raman spectroscopy as the Raman scattering of hydrogen produces a simple spectrum that is cleanly interpretable as a measurement of the orthohydrogen fraction. Also, neutron

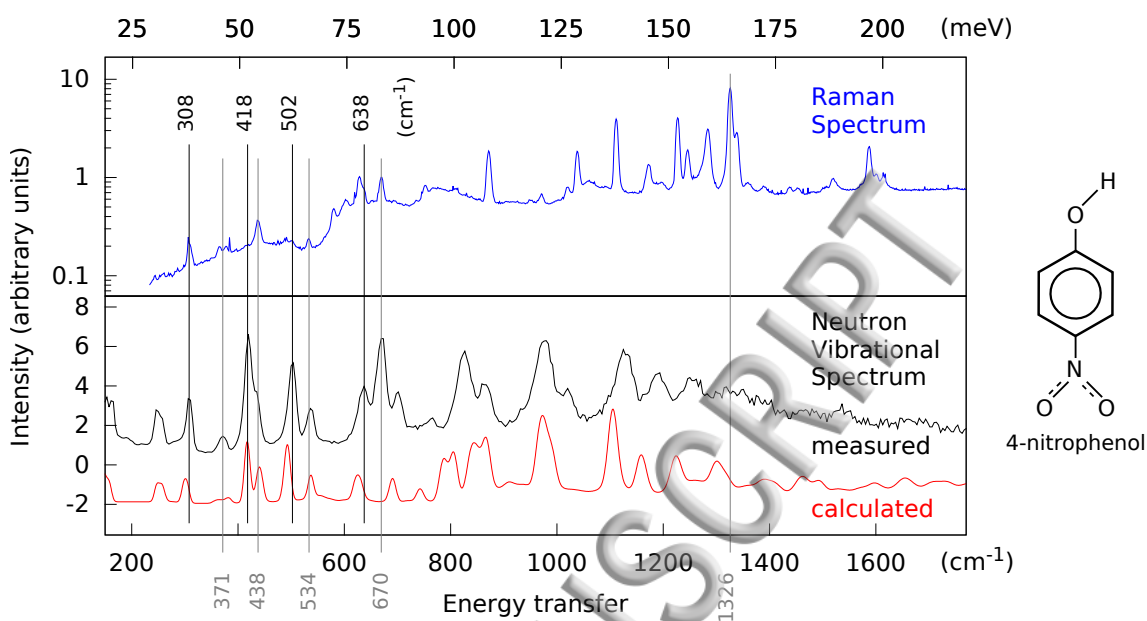


FIG. 4. Simultaneous Raman and neutron vibrational spectra of 4-nitrophenol at 20 K. The neutron data are from the backscattering detectors of VISION which are positioned at a scattering angle of 135°.

scattering is naturally suited for studying hydrogen, and the neutron vibrational spectrum of molecular hydrogen has a rich structure that is well complemented by the simplicity of its Raman spectrum.

A. The 4-Nitrophenol Study

Simultaneous Raman and neutron vibrational spectra of 4-nitrophenol are shown in Fig. 4. The complementarity of the two spectra is demonstrated by the fact that they are very different but share some similarities. Peaks are present in both spectra at around 308, 371, 438, 502, 534, 638 and 670 cm^{-1} energy transfer, but there are clear differences such as the fact that in the neutron spectrum the 438 cm^{-1} peak sits as a shoulder on a more intense peak that is either not present or is very weak in the Raman spectrum. Also, the two spectra are very different above 800 cm^{-1} energy transfer. The strongest peak of the Raman spectrum is at an energy transfer of about 1326 cm^{-1} . This excitation, which likely corresponds to what is given as the NO_2 symmetric stretch in Table 7 of Ref. 16, shows up dramatically in the Raman spectrum but is not visible in the neutron vibrational spectrum.

Also plotted in Fig. 4 is a simulation of the NVS spectrum. For details on how this simulation was conducted, please see the supplementary material. The reasonably good match between the simulation and the measurement allows us to assign the peaks to their corresponding vibrational modes. For example, the peaks below 600 cm^{-1} are mainly due to the deformation modes of the ring (twisting, distortion). Peaks in the range of 600 to 900 cm^{-1} can be attributed to the out-of-plane bending modes of the C-H bonds, as well as to the O-H torsion. From 900 to 1300 cm^{-1} , the in-plane bending modes of C-H and O-H start to appear. The NO_2 symmetric stretch is seen at about 1310 cm^{-1} in the simulation but does not produce a strong NVS peak due to the minimal involvement of hydrogen vibrations.

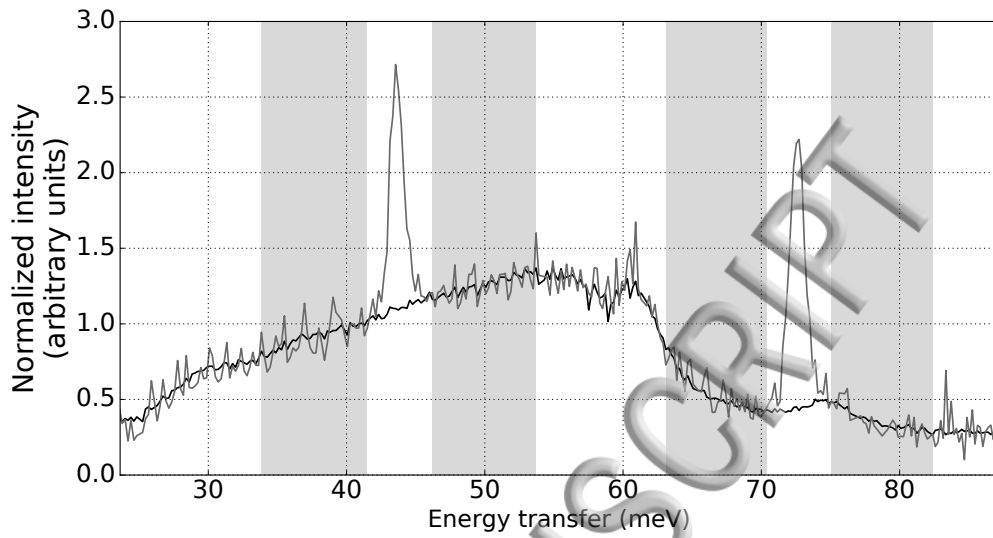


FIG. 5. A Raman spectrum of hydrogen (gray) and a background Raman spectrum (black) arising from scattering in the quartz rod. The hydrogen data shown here were taken from a liquid sample held at 17 K that had been mixed to have an orthohydrogen fraction of 72 %. The peak associated with scatter from parahydrogen can be seen at 43.9 meV and the peak associated with scatter from orthohydrogen can be seen at 72.8 meV.

B. The Hydrogen Study

In our second study, we measured simultaneous Raman and neutron vibrational spectra of a number of different samples of liquid and solid hydrogen of different orthohydrogen fractions. For some discussions on the topic of ortho- and parahydrogen, see e.g. Ref. 17–20. A summary of aspects of the topic of ortho- and parahydrogen that are relevant to our study is provided in the supplementary material.

The samples were prepared for this study by combining hydrogen in variable ratios from two sources: 1) a cylinder of hydrogen held at room temperature; and 2) hydrogen that had been sitting at low temperature inside an ortho-parahydrogen converter in contact with the ortho-parahydrogen conversion catalyst Oxisorb. To control and measure the mass of hydrogen loaded to the sample container, the hydrogen was intermediately loaded to a one-liter stainless steel dosing bottle at room temperature, and the pressure in this bottle was measured with a pressure transducer. Hydrogen was loaded to the sample in pressures of about one bar per dose, and from there was allowed to condense into the sample container which was held at 17 K. This dosing procedure was repeated until the desired masses and relative concentrations from the two sources had been condensed in the sample container. The preparation of a sample involved ten to twelve loadings of the dosing bottle and took about half an hour.

The temperature of the Oxisorb catalyst was held at 17 K, but was increased to 24 K during loading of the dosing bottle to raise the vapor pressure of the hydrogen in the converter. The thermal equilibrium orthohydrogen fractions of 17 K and 24 K hydrogen are 0.2 % and 0.7 % respectively. At room temperature, it is close to 75 %. About three minutes after having completed each sample preparation, simultaneous neutron and Raman spectra were taken at 17 K to observe the sample in the liquid state. For all but one of the mixtures, the hydrogen was subsequently cooled to 10 K to also observe a spectrum of the sample in the solid state. The Raman spectrum is not expected to be significantly different between the liquid and solid samples, but the neutron vibrational spectra have

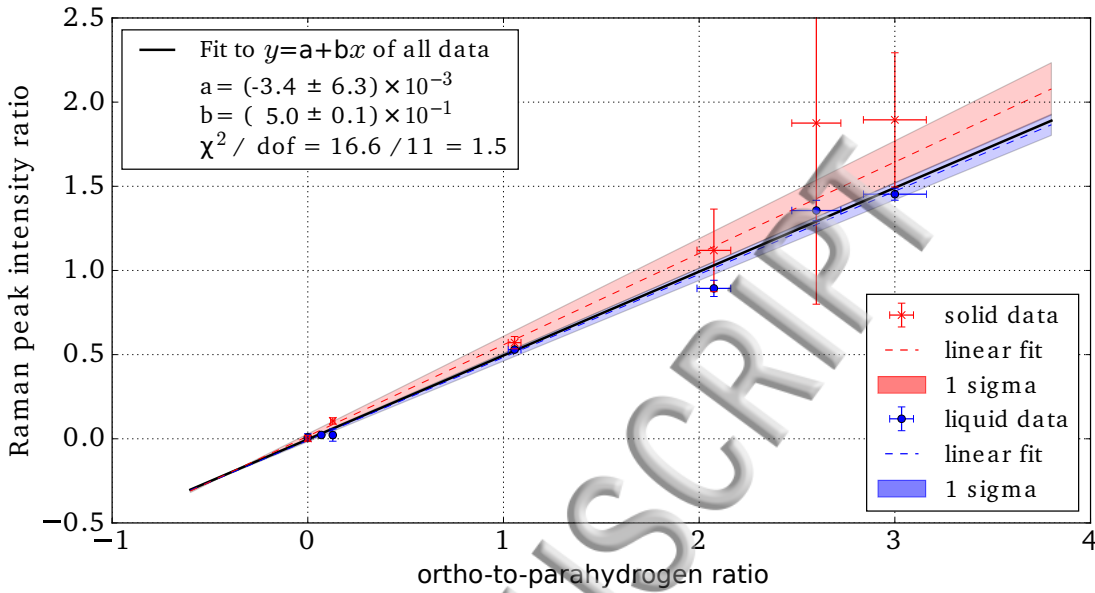


FIG. 6. The peak intensity ratio $S(1 \rightarrow 3)/S(0 \rightarrow 2)$ plotted versus the nominal ortho-to-parahydrogen ratio $(1 - c_e)/c_e$ that is expected based on the mixture used during the sample preparation. $S(1 \rightarrow 3)$ is the intensity of the peak associated with scatter from orthohydrogen, $S(0 \rightarrow 2)$ is the intensity of the peak associated with scatter from parahydrogen, and c_e is the expected parahydrogen fraction.

more well-defined features in the case of the solid.

A plot of the Raman spectrum of a sample of liquid hydrogen is given in Fig. 5. The two well-known lowest Stokes lines, one at 43.9 meV that is associated with scatter from parahydrogen and the other at 72.8 meV which is associated with scatter from orthohydrogen,^{18,21-23} are clearly visible and separable. Also shown in Fig. 5 is a measurement of the background due to the presence of the quartz rod. This background measurement was conducted using the same setup as for the hydrogen measurements, but with the sample container evacuated. For the background to be subtracted from the hydrogen signal, a linear fit was performed within the shaded region of one spectrum to the other to determine what is primarily a multiplicative normalization factor. Fig. 5 shows these two spectra after the relative normalization has been performed.

Fig. 6 shows the result of an analysis to test the correspondence between the ratio of intensities of the two Raman peaks and the ortho-to-parahydrogen ratio expected from the sample preparation procedure. This exercise was intended as a consistency check and first test of the Raman center stick, not as a calibration. The peak intensities were determined as the integral of the difference between pairs of spectra of the type shown in Fig. 5. The integral was conducted over the unshaded region of a given peak, and its uncertainty was determined from the standard deviation of this difference over the shaded regions surrounding the peak.

The uncertainty in the Raman peak areas was limited by large levels of nonstatistical electronic noise present in the optical spectrometer. In future we plan to use a newer spectrometer or refurbish the current one, and expect that the electronic noise will then be reduced considerably. The uncertainty in the summation over spectrometer pixels was assumed to scale as \sqrt{n} where n is the number of pixels over which the summation was conducted. The uncertainty in the measurement of the hydrogen masses was taken to be 30 mbar per fill of the dosing volume. Uncertainties in the Raman peak intensities are large for some of the solid samples. In these cases, the Raman signal was weak, which may have been

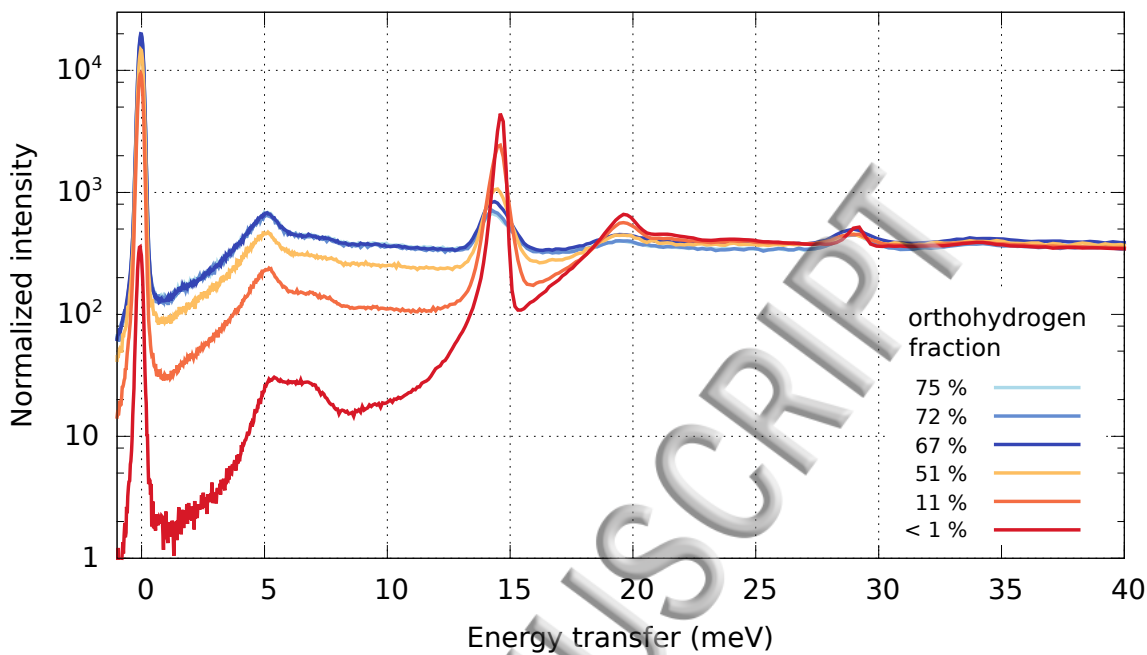


FIG. 7. Neutron vibrational spectra of solid hydrogen at a range of orthohydrogen fractions. These data are from the forward-scattering detectors which are arranged at a scattering angle of 45° . The orthohydrogen fractions stated in the legend are the values expected based on the mixture used during the sample preparation. Since the fraction of the sample mass viewed by the neutron beam varies, these spectra have been normalized to the ratio of the expected parahydrogen fraction to the area under the 14.7 meV peak.

due to the hydrogen having redistributed itself onto the side walls of the sample container as it was frozen (the side walls of the sample container were out of view of the optics but still in the neutron beam).

A straight line fit to the data of Fig. 6 is expected to have a dimensionless slope of 0.58 and zero intercept.^{18,24} A discussion of the origin of this number is given in the supplementary material. The observed intercept is consistent with zero, and the quality of the fit is quite good. The slope is about 15 % less than the expected number. This difference could be accounted for by downconversion of a few percent of the room temperature hydrogen as it was added to the sample container. However, this explanation is inconsistent with the fact that we did not observe conversion during the time that we were taking the Raman and neutron vibrational data. The discrepancy could also be explained by a wavelength-dependent property of the calibration of the optical spectrometer that we have yet to account for.

Fig. 7 shows NVS spectra of the solid form of the samples for which the Raman data are summarized in Fig. 6. A comparison of Fig. 5 and Fig. 7 demonstrates the contrast between the simplicity of the Raman spectrum of hydrogen and the richness of the NVS spectrum of hydrogen. The dependence of the NVS spectrum on the orthohydrogen fraction can be understood to a large extent by considering the rotational quantum numbers involved in producing a given spectral feature. For a discussion on this topic, please see the supplementary material.

IV. CONCLUSION

We have designed and built a center stick that allows for Raman spectroscopy to be performed simultaneously with the NVS measurements that are performed on the VISION neutron vibrational spectrometer of the SNS. This center stick could also be used on other instruments that have compatible sample-containment and sample environment requirements. In this paper, we have described the construction of this center stick and have presented the first spectra observed with its use.

This Raman center stick incorporates the cryogenic and vacuum requirements necessary for holding a material sample at temperatures down to about 5 K in the VISION cryogenic refrigerator. It includes an interface for connecting the sample container to a vacuum system, to a gas handling system, to cryogenic temperature monitoring and control, and it has optical connections for the excitation laser and the optical spectrometer. The optical components that direct and filter the light are held in an evacuated chamber, in physical proximity to the sample and within the cryogenic volume that holds samples at low temperature on VISION.

As a demonstration of this equipment, we have performed simultaneous observations of Raman and neutron vibrational spectra of 4-nitrophenol, and of solid and liquid hydrogen of a number of different orthohydrogen fractions. In addition to providing a test of this equipment, these studies have provided a demonstration of the complementarity of the two types of spectroscopy for which it is used.

V. SUPPLEMENTARY MATERIAL

For details on how the 4-nitrophenol simulation was conducted, for a short summary of aspects of orthohydrogen and parahydrogen that are relevant to our study, or for a discussion of the solid hydrogen NVS spectra, please see supplementary material.

VI. ACKNOWLEDGEMENTS

This work was sponsored by the Laboratory Directed Research and Development Program of Oak Ridge National Laboratory. It used resources at the Spallation Neutron Source, a U.S. Department of Energy Office of Science User Facility that is operated by Oak Ridge National Laboratory. Oak Ridge National Laboratory is managed by UT-Battelle, LLC, for the U.S. Department of Energy.

The authors would like to thank Luke Daemen and Anibal J. (Timmy) Ramirez-Cuesta of VISION for their extensive advice and expertise. We would also like to thank Neelam Pradhan, June Safieh and John Wenzel of the SNS Sample Environment Research and Development team for producing the design drawings and communicating with fabricators of the vacuum chamber and sample container referred to in this paper.

VII. REFERENCES

- ¹P C H Mitchell, S F Parker, A J Ramirez-Cuesta, J Tomkinson, *Vibrational Spectroscopy with Neutrons: with applications in Chemistry, Biology, Materials Science and Catalysis*, World Scientific Publishing Co. Pte. Ltd., Singapore, 2005
- ²B S Hudson, *Vibrational Spectroscopy* **42** (2006) 25–32
- ³G J Kearley, M R Johnson, *Vibrational Spectroscopy* **53** (2010) 54–59
- ⁴S F Parker, D Lennon, P W Albers, *Applied Spectroscopy* **65** (2011) 1325–1341
- ⁵I Kuliszewicz-Bajer, G Louarn, D Djurado, L Skorka, M Szymanski, J Y Mevellec, S Rols, A Pron, *The Journal of Physical Chemistry B*, **118** (2014) 5278–5288
- ⁶M A Adams, S F Parker, F Fernandez-Alonso, D J Cutler, C Hodges, A King, *Applied Spectroscopy* **63** (2009) 727–732

⁷P A Seeger, L L Daemen, J Z Larese, *Nuclear Instruments and Methods in Physics Research Section A* **604** (2009) 719–728

⁸Thorlabs, 56 Sparta Ave, Newton, NJ 07860

⁹J D Weiss, J H Stoever, *Applied Optics*, **24** (1985) 2755–2756

¹⁰E R I Abraham, E A Cornell, *Applied Optics* **37** (1998) 1762–1763

¹¹D L Miller, N T Moshegov, *Journal of Vacuum Science and Technology A* **19** (2001) 386–387

¹²J S Cowpe, R D Pilkington, *Vacuum* **82** (2008) 1341–1343

¹³B Buchholz, V Ebert, *Review of Scientific Instruments* **85** (2014) 055109

¹⁴Modu-Laser, 1258 West 50 South, Centerville, UT 84014

¹⁵Ocean Optics, 830 Douglas Avenue, Dunedin, FL 34698

¹⁶T Tanaka, A Nakajima, A Watanabe, T Ohno, Y Ozaki, *Vibrational Spectroscopy* **34** (2004) 157–167

¹⁷A Farkas, *Orthohydrogen, Parahydrogen and Heavy Hydrogen*, Cambridge University Press, London, U.K., 1935

¹⁸I F Silvera, *Reviews of Modern Physics* **52** (1980) 393–452

¹⁹P J Wheatley, *The Chemical Consequences of Nuclear Spin*, North Holland Publishing Company, Amsterdam, Netherlands, 1970

²⁰B A Tom, S Bhasker, Y Miyamoto, T Momose, B J McCall, *Review of Scientific Instruments* **80** (2009) 016108

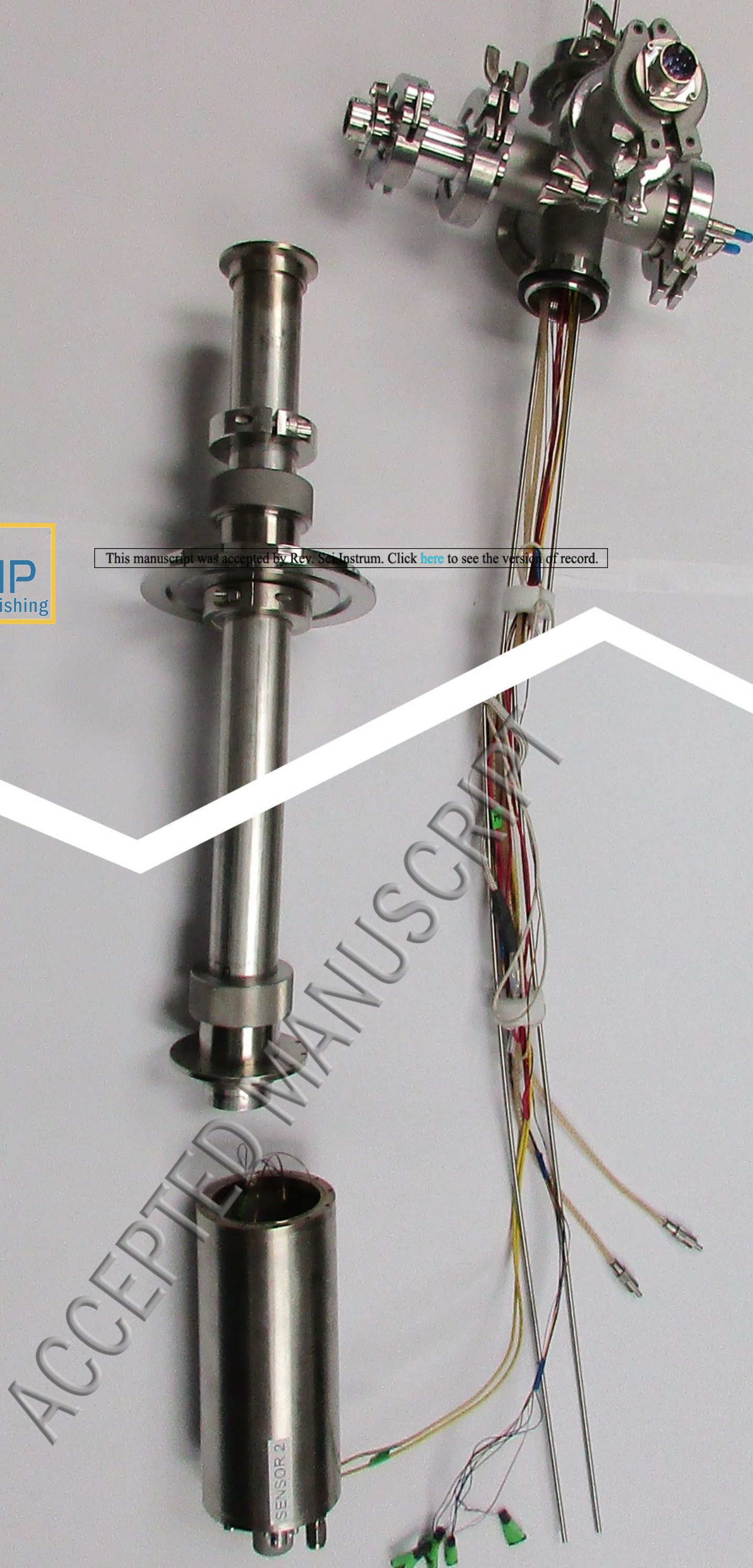
²¹Gerhard Herzberg, *Molecular Spectra and Molecular Structure: I. Spectra of Diatomic Molecules*, Volume 1, Second Edition, Van Nostrand Reinhold Company, New York, NY, 1950

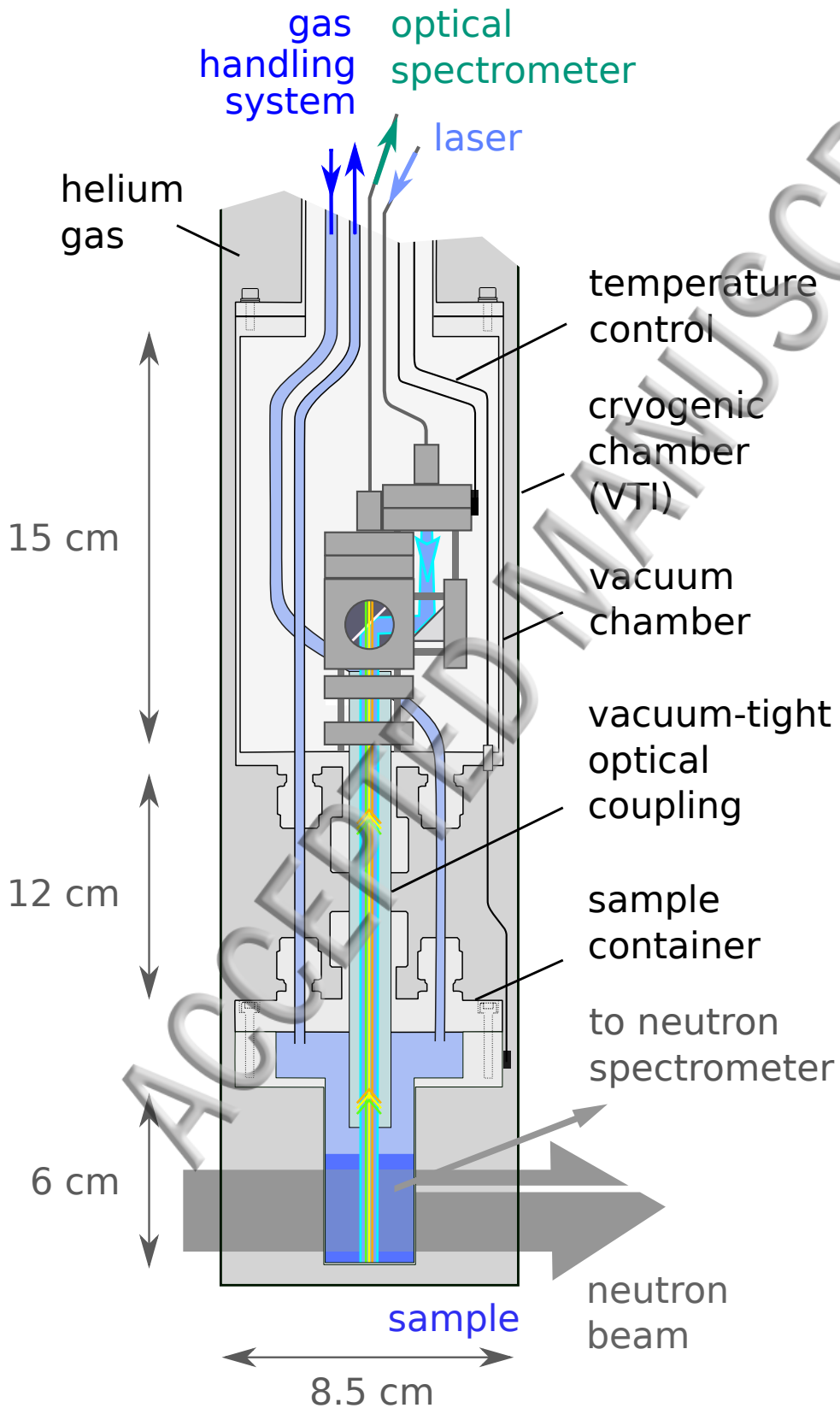
²²B P Stoicheff, *Canadian Journal of Physics*, **35** (1957) 730–741

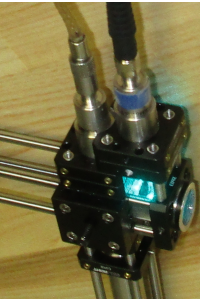
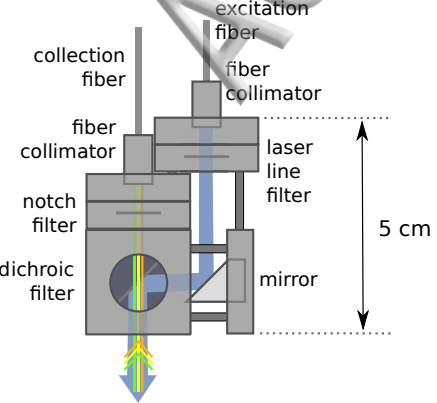
²³L Wolniewicz, *The Journal of Chemical Physics*, **45** (1966) 515–523

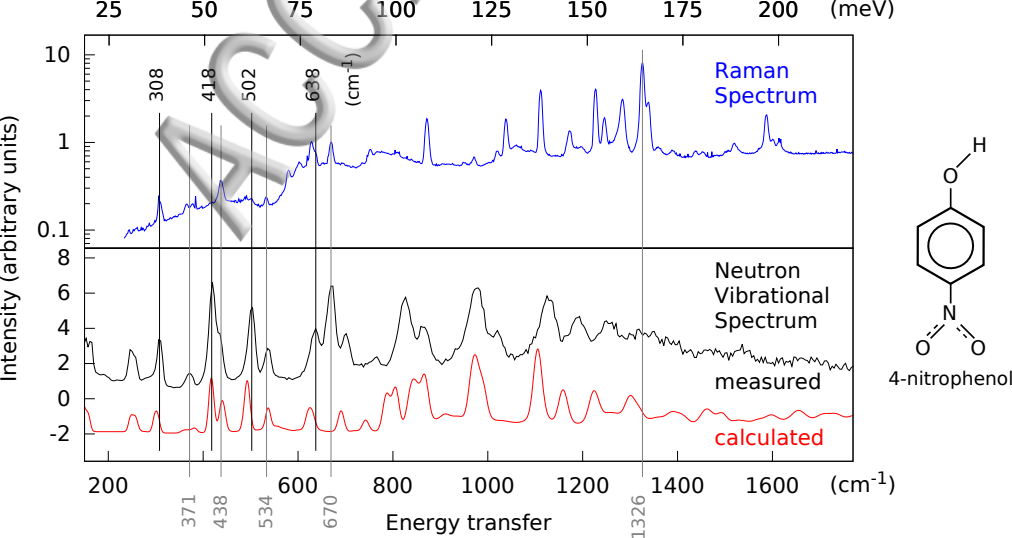
²⁴A Driessen, E van der Poll, I F Silvera, *Physical Review B* **30** (1984) 2517–2526

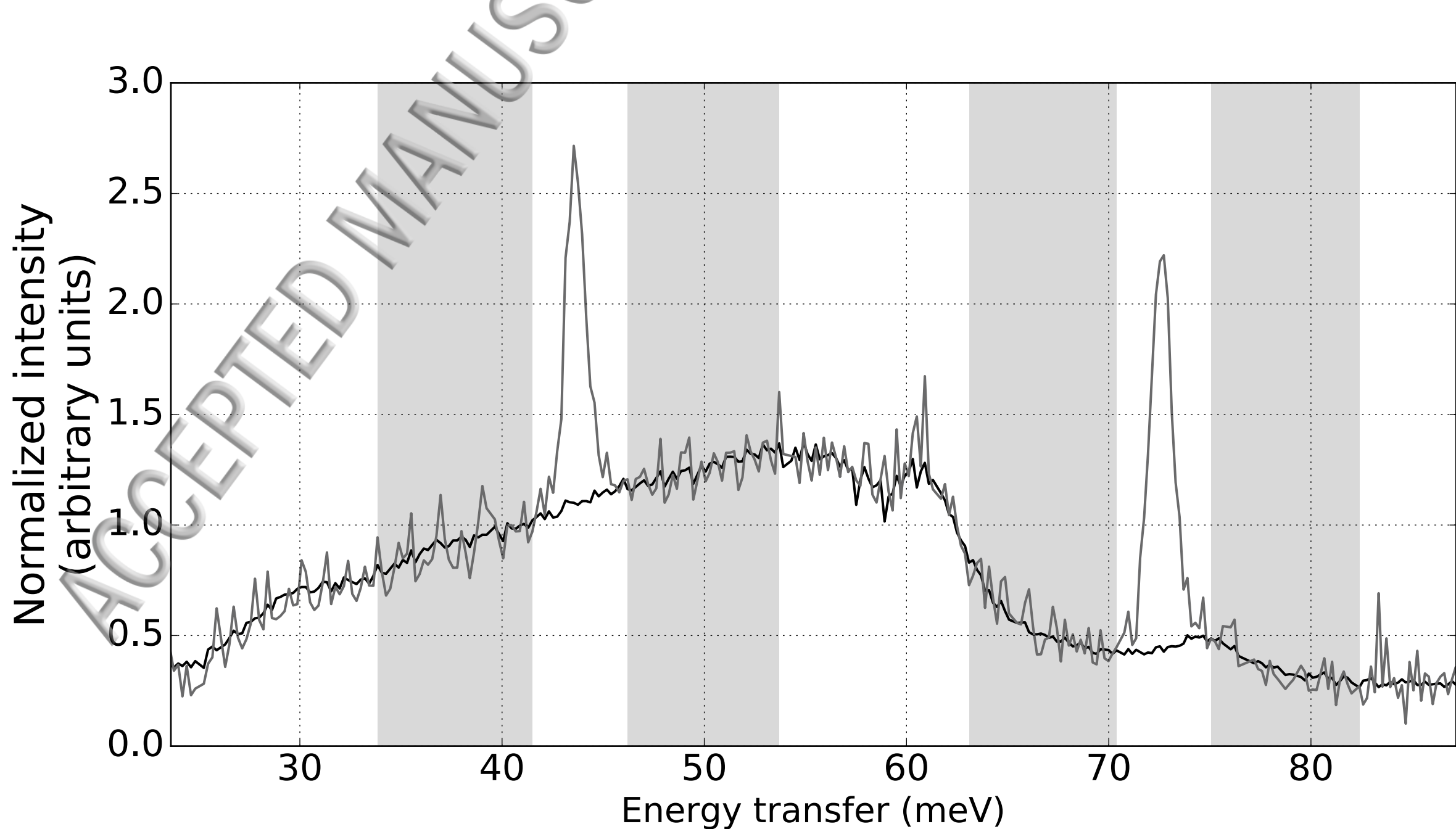
This manuscript was accepted by Rev. Sci. Instrum. Click [here](#) to see the version of record.











Accepted Manuscript

Raman peak intensity ratio

